

## Extensive Multipartite Entanglement from $su(2)$ Quantum Many-Body Scars

Jean-Yves Desaulès<sup>1</sup>, Francesca Pietracaprina<sup>2</sup>, Zlatko Papić<sup>1,\*</sup>, John Goold<sup>2,†</sup> and Silvia Pappalardi<sup>3,‡</sup>

<sup>1</sup>*School of Physics and Astronomy, University of Leeds, Leeds LS2 9JT, United Kingdom*

<sup>2</sup>*Department of Physics, Trinity College Dublin, D02PN40 Dublin 2, Ireland*

<sup>3</sup>*Laboratoire de Physique de l'École Normale Supérieure, ENS, Université PSL, CNRS, Sorbonne Université, Université de Paris, F-75005 Paris, France*

 (Received 4 October 2021; revised 3 May 2022; accepted 23 May 2022; published 5 July 2022)

Recent experimental observation of weak ergodicity breaking in Rydberg atom quantum simulators has sparked interest in quantum many-body scars—eigenstates which evade thermalization at finite energy densities due to novel mechanisms that do not rely on integrability or protection by a global symmetry. A salient feature of some quantum many-body scars is their subvolume bipartite entanglement entropy. In this Letter, we demonstrate that such exact many-body scars also possess extensive *multipartite* entanglement structure if they stem from an  $su(2)$  spectrum generating algebra. We show this analytically, through scaling of the quantum Fisher information, which is found to be superextensive for exact scarred eigenstates in contrast to generic thermal states. Furthermore, we numerically study signatures of multipartite entanglement in the PXP model of Rydberg atoms, showing that extensive quantum Fisher information density can be generated dynamically by performing a global quench experiment. Our results identify a rich multipartite correlation structure of scarred states with significant potential as a resource in quantum enhanced metrology.

DOI: [10.1103/PhysRevLett.129.020601](https://doi.org/10.1103/PhysRevLett.129.020601)

*Introduction.*—Beyond fundamental importance in quantum information theory [1], entanglement now plays a central role in many-body physics [2–4]. For example, the finite-size scaling of bipartite entanglement allows one to deduce important information on critical scalings in many-body systems [5], and through the identification of area and volume law behavior it can tell us about the feasibility of classical simulation. Entanglement is also central to the foundations of statistical mechanics [6]. Because of advances in experimental ultracold atomic physics, significant effort has been made to understand how quantum systems thermalize in the long-time limit [7–9]. Thermalizing systems which obey the eigenstate thermalization hypothesis (ETH) [8,10–12] have eigenstates that obey a volume law entanglement entropy. This agrees with common intuition that the highly excited energy eigenstates of many body systems are close to random vectors in the Hilbert space and as such should be highly entangled [13]. Volume-law bipartite entanglement entropy, therefore, is ubiquitous in nature. Unfortunately, this structure of bipartite entanglement is not known to lead to any practical advantage for quantum-enhanced technologies.

There are many facets to entanglement theory and, in particular, many-body systems offer the perfect playground to explore multipartite entanglement. In this Letter we focus on the multipartite structure in the eigenstates of complex many-body systems as described by the quantum Fisher information (QFI) [14–16]. The latter quantifies the usefulness of the quantum state as a resource for quantum enhanced metrology and can be directly related to

multipartite entanglement [17–19]. One particularly appealing feature of QFI is its relation to thermal susceptibilities [20–22], hence its experimental accessibility in condensed matter physics [20,23]. In fact, when computed for a thermal canonical Gibbs state the QFI can be written directly in terms of a Kubo response function [20]. This has led to experiments with neutron scattering [24,25] and experimental proposals in atomic platforms [26]. One may then ask the question, are there eigenstates of local many-body systems with an entanglement structure that could have operational significance for quantum information processing?

In this Letter, we demonstrate that systems with weak ergodicity breaking, possessing eigenstates known as quantum many-body scars (QMBS) [27,28], naturally realize a nontrivial form of extensive multipartite entanglement. QMBS are ETH-violating eigenstates which span a subspace that is effectively decoupled from the thermalizing bulk of the spectrum of a nonintegrable many-body system [29–31]. Such subspaces have been shown to arise due to several complementary mechanisms, including Hilbert space fragmentation [32–36] and projector embedding [37–40]. In this Letter, we focus on a large class of QMBS arising due to  $su(2)$  spectrum generating algebras [41–52]. The latter mechanism gives rise to an extensive number of QMBS eigenstates with equal energy spacing, leading to robust quantum revivals, usually from a simple product state. The  $su(2)$  QMBS are naturally realized in the so-called PXP spin model [53–59], in which signatures of QMBS have been observed experimentally [60,61].

While previous studies of QMBS have focused extensively on their bipartite entanglement, demonstrating an ETH violation via the subvolume law entanglement entropy, the study of *multipartite* entanglement of QMBS has so far been lacking. We show that exact  $\text{su}(2)$  QMBS have QFI that scales superextensively with system size, in contrast to generic thermal states of locally interacting Hamiltonians. Furthermore, remnants of this nontrivial scaling can be detected using dynamical quench experiments in systems with approximate QMBS, as we demonstrate numerically using the PXP model of Rydberg atoms [27]. As the QFI is related to the well-known response functions in condensed matter physics [20–22], this provides an opportunity for detection of multipartite entanglement in experiment and applications in quantum-enhanced sensing [62].

*Quantum Fisher information and multipartite entanglement.*—The QFI,  $\mathcal{F}_Q$ , is a central concept in quantum metrology that sets ultimate bounds on the precision on the estimation of a parameter [63]. The general goal is to estimate an unknown parameter  $\lambda$  using a quantum state  $\hat{\rho}$ . By performing a quantum measurement protocol, one finds the precision is constrained by the quantum Cramér-Rao bound  $(\Delta\lambda)^2 \geq 1/M\mathcal{F}_Q(\hat{\rho}_\lambda)$ , where  $M$  is the number of independent measurements made in the protocol,  $\hat{\rho}_\lambda$  is the state parametrized by  $\lambda$ , and  $\Delta\lambda$  is the variance [69,70]. The  $\mathcal{F}_Q$  admits an exact expression when the state  $\hat{\rho}_\lambda$  is generated by some Hermitian operator  $\hat{O}$  such that  $\hat{\rho}_\lambda = e^{i\lambda\hat{O}}\hat{\rho}e^{-i\lambda\hat{O}}$ . For a general mixed state, described by the density matrix  $\hat{\rho} = \sum_n p_n|n\rangle\langle n|$ , it reads [69]

$$\mathcal{F}_Q(\hat{O}, \hat{\rho}) = 2 \sum_{n,m} \frac{(p_n - p_m)^2}{p_n + p_m} |\langle n|\hat{O}|m\rangle|^2 \leq 4\langle\Delta\hat{O}^2\rangle, \quad (1)$$

with  $\langle\Delta\hat{O}^2\rangle = \text{Tr}(\hat{\rho}\hat{O}^2) - \text{Tr}(\hat{\rho}\hat{O})^2$ . The equality holds for pure states  $\hat{\rho} = |\psi\rangle\langle\psi|$ .

The QFI has key mathematical properties [15,69–71], such as convexity, additivity, monotonicity, and it can be used to probe the multipartite entanglement structure of a quantum state [17–19]. If, in a system with  $N$  particles and for a certain *collective* operator  $\hat{O} = \frac{1}{2}\sum_{i=1}^N \hat{o}_i$  (extensive sums of operators  $\hat{o}_i$  with local support), the QFI density satisfies the inequality

$$f_Q \equiv \frac{\mathcal{F}_Q(\hat{O}, \hat{\rho})}{N} > m, \quad (2)$$

then, at least  $(m+1)$  parties in the system are entangled (with  $1 \leq m \leq N-1$  a divisor of  $N$ ). Namely,  $m$  represents the size of the biggest entangled block of the quantum state. In particular, if  $N-1 \leq f_Q(\hat{O}) \leq N$ , then the state is called genuinely  $N$ -partite entangled.

*QFI of thermal eigenstates.*—In general, different operators  $\hat{O}$  lead to different bounds on QFI and there is no systematic method (without some knowledge on the physical

system [20,72]) to choose the optimal one. In this work, we restrict ourselves to one-dimensional systems and collective operators  $\hat{O} = \frac{1}{2}\sum_{i=1}^N \hat{o}_i$ , which are typically explored in cold-atom experiments and in interferometric schemes [70]. For the eigenstates  $|E_n\rangle$ , the QFI with respect to such collective operators  $\mathcal{F}_Q(\hat{O}, |E_n\rangle) = 4\langle E_n|\Delta\hat{O}^2|E_n\rangle$  can be expressed in terms of the connected correlation functions  $G_{i,j}(E_n) \equiv \langle E_n|\hat{o}_i\hat{o}_j|E_n\rangle - \langle E_n|\hat{o}_i|E_n\rangle\langle E_n|\hat{o}_j|E_n\rangle$ . If we further assume *translational invariance*, then  $G_{i,j} = G_{|i-j|}$  and the QFI density (2) reads

$$f_Q(\hat{O}, |E_n\rangle) = G_0(E_n) + 2 \sum_{r=1}^{N-1} G_r(E_n). \quad (3)$$

Note that  $G_0(E_n) = \mathcal{O}(1)$  is always an intensive quantity [73], hence the scaling of  $f_Q$  depends on the behavior of  $G_r(E_n)$  as a function of the distance  $r$ .

We now study the scaling of the QFI density (3) for generic chaotic eigenstates of a locally interacting many-body Hamiltonian far from criticality, which are well known to obey ETH [12]. In this case, the connected correlation functions scale as

$$G_r(E_n) \sim c_r e^{-r/\xi}, \quad r \gg \xi, \quad (4)$$

where  $|c_r| = \mathcal{O}(1)$  is an intensive constant that depends on the operators and  $\xi$  is the correlation length at energy  $E_n$ . This is a consequence of the clustering property of connected correlation functions of local observables, which has been demonstrated for canonical thermal states [74]. Appealing to ETH [75], the same clustering property holds for eigenstates of local Hamiltonians up to subextensive corrections [76]. The decay of correlations in Eq. (4) holds despite the volume-law entanglement entropy of the eigenstates [77–79], see the discussion in [63] and Refs. [54,80] for numerical examples.

By plugging Eq. (4) into Eq. (3) and summing over  $r$ , we obtain for  $N \gg 1$

$$f_Q(\hat{O}, |E_n\rangle) \lesssim G_0(E_n) + \frac{2c}{e^{1/\xi} - 1} + \mathcal{O}(e^{-N}), \quad (5)$$

where we have used  $|c_r| \leq c = \mathcal{O}(1)$ . This equation shows that generically the QFI density of chaotic eigenstates, away from criticality, is an intensive quantity that can be evaluated explicitly from the knowledge of the thermal correlation length. Furthermore, whenever the correlation length  $\xi$  is large (but finite), one has

$$f_Q(\hat{O}, |E_n\rangle) \simeq 2\xi \quad \text{for } \xi \gg 1. \quad (6)$$

Thus, the QFI is also large and finite. By comparing this expression with the relation to multipartite entanglement (2), we find that the size of the biggest entangled block

scales as twice the correlation length. This finding is fully consistent with known results for critical pure or thermal states, where the QFI for the order parameter diverges universally [20,22,81–84].

As a side note, the above result for pure chaotic eigenstates satisfying ETH can be compared with that for QFI of thermal states [20] (or the asymptotic state of a quenched dynamics). In the latter case, the QFI bounds from above the corresponding canonical expression the Gibbs state  $\mathcal{F}(\hat{O}, |E\rangle) \geq \mathcal{F}(\hat{O}, \hat{\rho}_{\text{Gibbs}})$  [22].

*QFI of exact scars.*—We next contrast the scaling of the QFI for thermal eigenstates (5) to the one for a class of *exact* QMBS. More precisely, we focus our work on scarred eigenstates that can be described within the general framework of Mark, Lin, and Motrunich [43] (see also Ref. [44]). Whenever there exists a linear subspace  $W \subset \mathcal{H}$  of the Hilbert space and an operator  $\hat{Q}^\dagger$  such that  $\hat{Q}^\dagger W \subset W$  and

$$([\hat{H}, \hat{Q}^\dagger] - \omega \hat{Q}^\dagger)W = 0, \quad (7)$$

then the Hamiltonian admits the following exact eigenstates  $|\mathcal{S}_n\rangle$  and corresponding eigenvalues  $E_n$ ,

$$|\mathcal{S}_n\rangle = (\hat{Q}^\dagger)^n |\mathcal{S}_0\rangle, \quad E_n = E_0 + n\omega, \quad (8)$$

where  $|\mathcal{S}_0\rangle$  is an eigenstate of the Hamiltonian  $\hat{H}$  with eigenvalue  $E_0$ . In other words,  $\hat{Q}^\dagger$  is a dynamical symmetry of the Hamiltonian restricted to the subspace  $W$ . The specific form of the operator  $\hat{Q}^\dagger$  is model dependent. Typically, it is a collective operator with momentum  $\pi$ , e.g., in one dimension  $\hat{Q}^\dagger = \sum_{i=1}^N (-1)^i \hat{\sigma}_i$  with  $\hat{\sigma}_i$  an operator with local support [43]. Note that Eq. (8) implies equal energy spacing among the scarred eigenstates, and so any state that would have overlap only on these states would show perfect wave function revivals. Let us define

$$\hat{J}^+ \equiv \frac{\hat{Q}^\dagger}{2}, \quad \hat{J}^- \equiv \frac{\hat{Q}}{2}, \quad \hat{J}^z \equiv \frac{\hat{H}}{\omega}, \quad (9)$$

which forms the Cartan-Weyl basis of an  $\text{su}(2)$  algebra. We will use the following notation  $\hat{A} =_w \hat{B}$  meaning that the equality holds only on the subset  $W$  (8). For instance, Eq. (7) reads  $[\hat{J}^z, \hat{J}^\pm] =_w \pm \hat{J}^\pm$ .

Depending on how the algebra is completed, one may obtain different results on the scaling of correlations. If, for instance, one has  $[\hat{J}^+, \hat{J}^-] = 1$ —the standard algebra of the harmonic oscillator—then  $\hat{J}^\pm$  act like creation and annihilation operators, while  $\hat{J}^+ \hat{J}^-$  acts as a number operator. It follows

$$\frac{\langle \mathcal{S}_n | \hat{J}^+ \hat{J}^- | \mathcal{S}_n \rangle}{N^2} = \frac{1}{N} \frac{n}{N}, \quad (10)$$

and there cannot be any long-range order. Suppose, instead, that the operators  $\hat{J}$  obey

$$[\hat{J}^+, \hat{J}^-] =_w 2\hat{J}^z. \quad (11)$$

For such an algebraic structure one can show [63]

$$\frac{\langle \mathcal{S}_n | \hat{J}^+ \hat{J}^- | \mathcal{S}_n \rangle}{N^2} = \frac{2\epsilon_0}{\omega} \frac{n}{N} - \left(\frac{n}{N}\right)^2 + \frac{n}{N^2}, \quad (12)$$

where  $\epsilon_0$  is the ground state energy density, i.e.,  $E_0 = -N\epsilon_0$ . As  $n = 0$  to  $N$ , the first two terms are  $\mathcal{O}(1)$  while the last one is only  $\mathcal{O}(1/N)$ .

Hence, exact scars with finite energy density [ $n/N = \mathcal{O}(1)$ ] possess *long-range order* [85]. As such, for the local operators  $\hat{\sigma}_i$  appearing in  $\hat{Q}^\dagger$ , the connected correlation functions are finite in the thermodynamic limit (13), i.e.,

$$G_r(E_n) \sim \text{const}, \quad r \rightarrow \infty, \quad N \rightarrow \infty. \quad (13)$$

This property was used in Ref. [54] to interpret scarred eigenstates as finite-energy-density condensates of weakly interacting  $\pi$  magnons that possess long-range order in both space and time. A key result of our findings is that, through Eq. (3), the presence of long-range order implies genuine multipartite entanglement of this class of QMBS. In fact, the QFI density with respect to the operators  $\hat{J}^x = (\hat{J}^+ + \hat{J}^-)/2$  reads

$$f_Q(\hat{J}^x, |\mathcal{S}_n\rangle) = 2 \left( \frac{2\epsilon_0}{\omega} - \frac{n}{N} \right) n + \frac{2\epsilon_0}{\omega}, \quad (14)$$

where we used  $\langle \mathcal{S}_n | \hat{J}^x | \mathcal{S}_n \rangle = \langle \mathcal{S}_n | (\hat{J}^\pm)^2 | \mathcal{S}_n \rangle = 0$  to get rid of all terms except the ones in Eq. (12). Therefore exact scars with finite energy density  $n \sim N$  possess superextensive QFI  $F_Q \sim N^2$  and they are genuinely multipartite entangled. In general, it is highly nontrivial to engineer superextensive scaling of quantum Fisher information for many-body states [71]. The identification of such states as a subspace in the spectrum of physical, locally interacting systems is our central result.

*Experimental implications for Rydberg atoms.*—Signatures of QMBS have been observed in experiments on Rydberg-blockaded atomic chains [60] and Bose-Hubbard quantum simulators [61]. Denoting by  $|\circ\rangle$  and  $|\bullet\rangle$  the ground and excited states of each atom, respectively, the effective ‘‘PXP’’ Hamiltonian describing such systems is given by [86,87]

$$\hat{H} = \Omega \sum_j \hat{P}_{j-1} \hat{X}_j \hat{P}_{j+1}, \quad (15)$$

where  $\hat{X} = |\circ\rangle\langle\bullet| + |\bullet\rangle\langle\circ|$  is the Pauli operator,  $\hat{P} = |\circ\rangle\langle\circ|$  is the projector on the ground state of an atom,

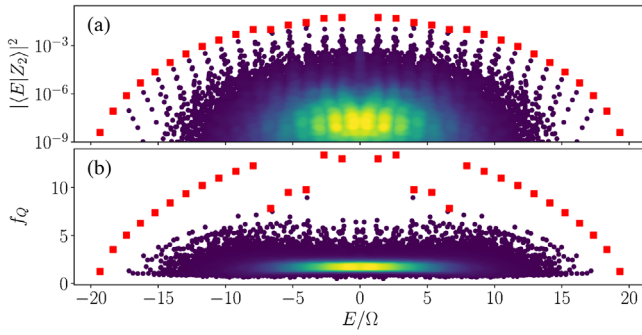


FIG. 1. (a) Overlap between exact PXP eigenstates and the Néel state. Red squares indicate the QMBS eigenstates. (b) The QFI density of the PXP eigenstates. The red squares denote the same QMBS eigenstates as in (a). In both plots, the dips in the middle of the spectrum are due to hybridization of QMBS eigenstates with thermal states. The color code indicates the density of points and all data are for the PXP model in Eq. (15) with  $N = 32$  spins.

and  $\Omega$  is the Rabi frequency. We also assume periodic boundary conditions. The Hamiltonian in Eq. (15) is compatible with the Rydberg blockade constraint as it allows an atom to change state only if both of its neighbors are in the ground state, thus neighboring excitations such as  $|\dots\bullet\bullet\dots\rangle$  are excluded.

While the model in Eq. (15) is nonintegrable and thermalizing [27], when quenched from the Néel product state of atoms,  $|\mathbb{Z}_2\rangle = |\bullet\circ\bullet\circ\dots\rangle$ , long-lived oscillations are seen in the dynamics of entanglement entropy and local observables [27,53,60]. This is despite the  $|\mathbb{Z}_2\rangle$  state being effectively at “infinite temperature.” The origin of these oscillations is a set of  $N + 1$  QMBS eigenstates [27] that form an approximate  $\text{su}(2)$  algebra [88,89]. However, this algebra is only approximate, hence Eq. (7) is not exactly obeyed; moreover, the algebra involves nonlocal generators, hence it is not easy to directly measure. To circumvent this problem, we employ the alternating magnetic field operator,

$$\hat{M}_S = \frac{1}{2} \sum_j (-1)^j \hat{Z}_j, \quad (16)$$

where  $\hat{Z} = |\bullet\rangle\langle\bullet| - |\circ\rangle\langle\circ|$ . This operator is natural because it is experimentally accessible and it is proportional to the total spin  $\hat{J}^x$  operator in the approximate  $\text{su}(2)$  algebra of Ref. [54], while QMBSs are eigenstates of the corresponding  $\hat{J}^z$  operator, defined via Eq. (11).

Figure 1 shows that, as for exact scars, the QMBS eigenstates in the PXP model have largest QFI among all eigenstates. Further differences in the connected correlation functions between QMBS and other thermalizing eigenstates are also observed [63]. However, as the scarred PXP subspace is weakly connected to the rest of the Hilbert space, in larger systems the QMBS eigenstates begin to hybridize with thermal eigenstates [53], which is

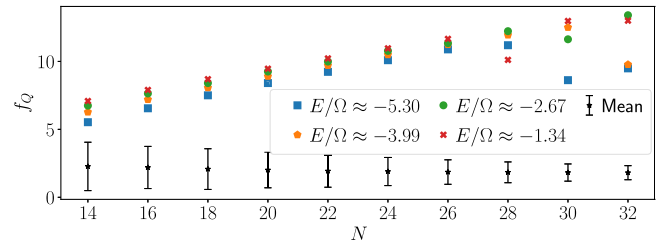


FIG. 2. Finite size scaling of QFI density for several QMBS eigenstates of the PXP model with energies  $E$  near the middle of the spectrum, contrasted against the mean value over all eigenstates. The scaling is extensive until  $N = 28$ , where hybridization between the scarred eigenstates and thermal eigenstates with a similar energy starts to lower  $f_Q$ .

manifested as a reduction in QFI and the overlap with the Néel state. Signatures of this in the middle of the spectrum can be observed in Fig. 1. Hybridization also prevents the QFI of the individual QMBS states to scale superextensively beyond a certain size, see Fig. 2. The same figure also shows that, for thermal eigenstates,  $f_Q$  does not depend on  $N$ , as predicted in Eq. (5).

While hybridization will likely prevent any single QMBS eigenstate from having a superextensive QFI,  $F_Q \propto N^2$ , in the asymptotic limit, such exact eigenstates cannot realistically be prepared in Rydberg atom experiments, as they lack protection from any global symmetry. Instead, we propose that extensive QFI in this model can be leveraged in practice by dynamically evolving the system to moderate times, i.e., times longer than the initial relaxation scale  $\sim 1/\Omega$ , where  $\Omega$  is the Rabi frequency for the model in Eq. (15). In Fig. 3 we computed the evolution of QFI density when the PXP model is quenched from various initial states, contrasting the behavior of  $|\mathbb{Z}_2\rangle$  with thermalizing initial states, such as the polarized state,  $|\circ\circ\circ\dots\rangle$ , and other random product states.

The dynamics from the  $|\mathbb{Z}_2\rangle$  state in Fig. 3 clearly stands out from other thermalizing initial states. Following the initial spreading,  $f_Q$  undergoes a fast growth in the  $|\mathbb{Z}_2\rangle$  case, reaching a broad maximum at intermediate times,  $O(10^2)$ . For all system sizes investigated (including the ones where eigenstate hybridization is observed), the value of this maximum is extensive in system size. Larger systems can also be investigated using the symmetric subspace approximation [59], confirming the extensive scaling within this framework [63]. At much later times, however,  $f_Q$  starts to drop, as expected from the eigenstate plot in Fig. 1. The nonextensivity of the late-time value of  $f_Q$  can be independently confirmed by computing the infinite-time average using the diagonal ensemble with corrections for higher moments [63].

Finally, we note that in addition to the tower of  $N + 1$  scarred eigenstates considered above, the PXP model also hosts a few isolated *exact* scar states near the middle of its spectrum [55]. The latter can be expressed as matrix

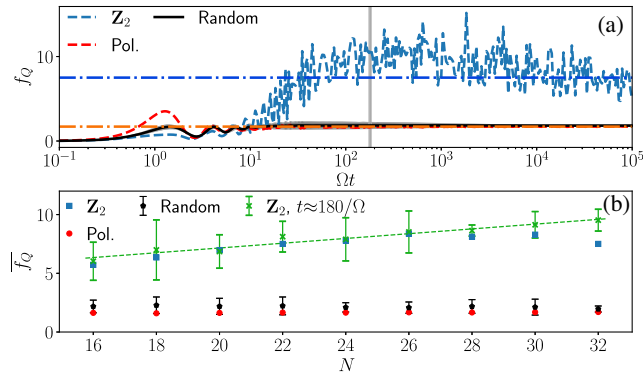


FIG. 3. (a) Time evolution of QFI density following quenches from various initial states. The horizontal lines show the infinite-time QFI density averages for the Néel state and the polarized state. (b) Infinite-time QFI density averages for various initial states as a function of system size. The green crosses correspond to the average over the time window indicated in gray in (a). Its width is longer than the revival period of the Néel state in order to average over these higher-frequency oscillations. The window is centered around  $t = 180/\Omega$ , because at this time the maximum has been reached for all system sizes investigated but the drop at even later times has not started yet. The dashed green line is a linear fit  $0.20N + 3.06$  to this data. In both plots the data for random states is an average over 20 samples and the error bars correspond to the standard deviation.

product states and therefore have area-law entanglement. One can prove [63] that for these states  $f_Q$  is bounded by a constant when probed with the alternating magnetic field [Eq. (16)], which makes such exact PXP scars distinct from both the approximate PXP scarred eigenstates as well as the towers of exact scars obeying the restricted spectrum generating algebra in Eq. (7).

*Discussion.*—In this Letter, we have analytically demonstrated that a large family of exact QMBS, described by Eqs. (7) and (8), can be distinguished from bulk thermal eigenstates through the scaling of their QFI. We find that the long-range order of QMBS implies the superextensive scaling of the QFI. This feature, together with the logarithmic scaling of the entanglement entropy, affirms the *semiclassical* nature of such states, that share the same entanglement properties of asymptotic semiclassical trajectories [64]. Moreover, our numerical study of the PXP model shows that robust signatures of superextensive QFI scaling can be expected despite the nonexact nature of QMBS in that model. We also provided evidence that this structure can be probed dynamically by measuring the variance of an appropriate operator in current Rydberg atom experiments. The multipartite entanglement considered here is very special and is known to have potential use for quantum enhanced metrology. Given this finding for QMBS, which are a particular example of weak-ergodicity breaking, it would be interesting to investigate if other systems in this class could show scaling of entanglement beyond bipartite correlations.

In compliance with EPSRC policy framework on research data, this publication is theoretical work that does not require supporting research data.

We thank Alessandro Silva for useful comments on the manuscript. S. P. and J. G. thank S. Gainsburg, J. Y. D. thanks Christopher Turner for useful comments on the diagonal ensemble. We acknowledge support by EPSRC Grants No. R020612/1 (Z. P.) and No. R513258/1 (J. Y. D.). Z. P. acknowledges support by the Leverhulme Trust Research Leadership Award No. RL-2019-015. J. G. is supported by a SFI-Royal Society University Research Fellowship and acknowledges funding from European Research Council Starting Grant ODYSSEY (Grant Agreement No. 758403). S. P. is supported by the Simons Foundation Grant No. 454943. F. P. has received funding from the European Union’s Horizon 2020 research and innovation programme under the Marie Skłodowska-Curie Grant No. 838773.

\*z.papic@leeds.ac.uk

†gooldj@tcd.ie

‡silvia.pappalardi@phys.ens.fr

- [1] R. Horodecki, P. Horodecki, M. Horodecki, and K. Horodecki, *Rev. Mod. Phys.* **81**, 865 (2009).
- [2] L. Amico, R. Fazio, A. Osterloh, and V. Vedral, *Rev. Mod. Phys.* **80**, 517 (2008).
- [3] N. Laflorencie, *Phys. Rep.* **646**, 1 (2016).
- [4] G. D. Chiara and A. Sanpera, *Rep. Prog. Phys.* **81**, 074002 (2018).
- [5] J. Eisert, M. Cramer, and M. B. Plenio, *Rev. Mod. Phys.* **82**, 277 (2010).
- [6] S. Popescu, A. J. Short, and A. Winter, *Nat. Phys.* **2**, 754 (2006).
- [7] M. Rigol, V. Dunjko, and M. Olshanii, *Nature (London)* **452**, 854 (2008).
- [8] L. D’Alessio, Y. Kafri, A. Polkovnikov, and M. Rigol, *Adv. Phys.* **65**, 239 (2016).
- [9] J. Eisert, M. Friesdorf, and C. Gogolin, *Nat. Phys.* **11**, 124 (2015).
- [10] M. Srednicki, *Phys. Rev. E* **50**, 888 (1994).
- [11] M. Srednicki, *J. Phys. A* **29**, L75 (1996).
- [12] M. Srednicki, *J. Phys. A* **32**, 1163 (1999).
- [13] D. N. Page, *Phys. Rev. Lett.* **71**, 1291 (1993).
- [14] C. W. Helstrom, *J. Stat. Phys.* **1**, 231 (1969).
- [15] G. Tóth and I. Apellaniz, *J. Phys. A* **47**, 424006 (2014).
- [16] L. Pezzè and A. Smerzi, arXiv:1411.5164.
- [17] P. Hyllus, W. Laskowski, R. Krischek, C. Schwemmer, W. Wieczorek, H. Weinfurter, L. Pezzè, and A. Smerzi, *Phys. Rev. A* **85**, 022321 (2012).
- [18] G. Tóth, *Phys. Rev. A* **85**, 022322 (2012).
- [19] L. Pezzè and A. Smerzi, *Phys. Rev. Lett.* **102**, 100401 (2009).
- [20] P. Hauke, M. Heyl, L. Tagliacozzo, and P. Zoller, *Nat. Phys.* **12**, 778 (2016).
- [21] S. Pappalardi, A. Russomanno, A. Silva, and R. Fazio, *J. Stat. Mech.* (2017) 053104.

- [22] M. Brenes, S. Pappalardi, J. Goold, and A. Silva, *Phys. Rev. Lett.* **124**, 040605 (2020).
- [23] H. Strobel, W. Muessel, D. Linnemann, T. Zibold, D. B. Hume, L. Pezzè, A. Smerzi, and M. K. Oberthaler, *Science* **345**, 424 (2014).
- [24] P. Laurell, A. Scheie, C. J. Mukherjee, M. M. Koza, M. Enderle, Z. Tylczynski, S. Okamoto, R. Coldea, D. A. Tennant, and G. Alvarez, *Phys. Rev. Lett.* **127**, 037201 (2021).
- [25] A. Scheie, P. Laurell, A. M. Samarakoon, B. Lake, S. E. Nagler, G. E. Granroth, S. Okamoto, G. Alvarez, and D. A. Tennant, *Phys. Rev. B* **103**, 224434 (2021).
- [26] R. Costa de Almeida and P. Hauke, *Phys. Rev. Research* **3**, L032051 (2021).
- [27] C. J. Turner, A. A. Michailidis, D. A. Abanin, M. Serbyn, and Z. Papić, *Nat. Phys.* **14**, 745 (2018).
- [28] W. W. Ho, S. Choi, H. Pichler, and M. D. Lukin, *Phys. Rev. Lett.* **122**, 040603 (2019).
- [29] M. Serbyn, D. A. Abanin, and Z. Papić, *Nat. Phys.* **17**, 675 (2021).
- [30] Z. Papić, [arXiv:2108.03460](https://arxiv.org/abs/2108.03460).
- [31] S. Moudgalya, B. A. Bernevig, and N. Regnault, [arXiv:2109.00548](https://arxiv.org/abs/2109.00548).
- [32] V. Khemani, M. Hermele, and R. Nandkishore, *Phys. Rev. B* **101**, 174204 (2020).
- [33] P. Sala, T. Rakovszky, R. Verresen, M. Knap, and F. Pollmann, *Phys. Rev. X* **10**, 011047 (2020).
- [34] S. Moudgalya, A. Prem, R. Nandkishore, N. Regnault, and B. A. Bernevig, *Memorial Volume for Shoucheng Zhang* (World Scientific, Singapore, 2021), Chap. 7, pp. 147–209.
- [35] A. Hudomal, I. Vasić, N. Regnault, and Z. Papić, *Commun. Phys.* **3**, 99 (2020).
- [36] H. Zhao, J. Vovrosh, F. Mintert, and J. Knolle, *Phys. Rev. Lett.* **124**, 160604 (2020).
- [37] N. Shiraishi and T. Mori, *Phys. Rev. Lett.* **119**, 030601 (2017).
- [38] S. Ok, K. Choo, C. Mudry, C. Castelnovo, C. Chamon, and T. Neupert, *Phys. Rev. Research* **1**, 033144 (2019).
- [39] J. Wildeboer, A. Seidel, N. S. Srivatsa, A. E. B. Nielsen, and O. Erten, *Phys. Rev. B* **104**, L121103 (2021).
- [40] F. M. Surace, G. Giudici, and M. Dalmonte, *Quantum* **4**, 339 (2020).
- [41] S. Moudgalya, N. Regnault, and B. A. Bernevig, *Phys. Rev. B* **98**, 235156 (2018).
- [42] M. Schechter and T. Iadecola, *Phys. Rev. Lett.* **123**, 147201 (2019).
- [43] D. K. Mark, C.-J. Lin, and O. I. Motrunich, *Phys. Rev. B* **101**, 195131 (2020).
- [44] S. Moudgalya, N. Regnault, and B. A. Bernevig, *Phys. Rev. B* **102**, 085140 (2020).
- [45] T. Iadecola and M. Schechter, *Phys. Rev. B* **101**, 024306 (2020).
- [46] N. Shibata, N. Yoshioka, and H. Katsura, *Phys. Rev. Lett.* **124**, 180604 (2020).
- [47] S. Chattopadhyay, H. Pichler, M. D. Lukin, and W. W. Ho, *Phys. Rev. B* **101**, 174308 (2020).
- [48] K. Lee, R. Melendrez, A. Pal, and H. J. Changlani, *Phys. Rev. B* **101**, 241111(R) (2020).
- [49] K. Pakrouski, P. N. Pallegar, F. K. Popov, and I. R. Klebanov, *Phys. Rev. Lett.* **125**, 230602 (2020).
- [50] J. Ren, C. Liang, and C. Fang, *Phys. Rev. Lett.* **126**, 120604 (2021).
- [51] N. O’Dea, F. Burnell, A. Chandran, and V. Khemani, *Phys. Rev. Research* **2**, 043305 (2020).
- [52] T. Comparin, F. Mezzacapo, and T. Roscilde, *Phys. Rev. A* **105**, 022625 (2022).
- [53] C. J. Turner, A. A. Michailidis, D. A. Abanin, M. Serbyn, and Z. Papić, *Phys. Rev. B* **98**, 155134 (2018).
- [54] T. Iadecola, M. Schechter, and S. Xu, *Phys. Rev. B* **100**, 184312 (2019).
- [55] C.-J. Lin and O. I. Motrunich, *Phys. Rev. Lett.* **122**, 173401 (2019).
- [56] N. Shiraishi, *J. Stat. Mech.* (2019) 083103.
- [57] C.-J. Lin, A. Chandran, and O. I. Motrunich, *Phys. Rev. Research* **2**, 033044 (2020).
- [58] I. Mondragon-Shem, M. G. Vavilov, and I. Martin, *PRX Quantum* **2**, 030349 (2021).
- [59] C. J. Turner, J.-Y. Desaulles, K. Bull, and Z. Papić, *Phys. Rev. X* **11**, 021021 (2021).
- [60] H. Bernien, S. Schwartz, A. Keesling, H. Levine, A. Omran, H. Pichler, S. Choi, A. S. Zibrov, M. Endres, M. Greiner *et al.*, *Nature (London)* **551**, 579 (2017).
- [61] G.-X. Su, H. Sun, A. Hudomal, J.-Y. Desaulles, Z.-Y. Zhou, B. Yang, J. C. Halimeh, Z.-S. Yuan, Z. Papić, and J.-W. Pan, [arXiv:2201.00821](https://arxiv.org/abs/2201.00821).
- [62] S. Dooley, *PRX Quantum* **2**, 020330 (2021).
- [63] See Supplemental Material at <http://link.aps.org/supplemental/10.1103/PhysRevLett.129.020601> for additional analysis and background calculations to support the results in the main text, which includes Refs. [64–68].
- [64] A. Leroze and S. Pappalardi, *Phys. Rev. A* **102**, 032404 (2020).
- [65] A. Pal and D. A. Huse, *Phys. Rev. B* **82**, 174411 (2010).
- [66] D. A. Abanin, E. Altman, I. Bloch, and M. Serbyn, *Rev. Mod. Phys.* **91**, 021001 (2019).
- [67] M. Schechter and T. Iadecola, *Phys. Rev. B* **98**, 035139 (2018).
- [68] V. Khemani, C. R. Laumann, and A. Chandran, *Phys. Rev. B* **99**, 161101(R) (2019).
- [69] S. L. Braunstein and C. M. Caves, *Phys. Rev. Lett.* **72**, 3439 (1994).
- [70] L. Pezzè, A. Smerzi, M. K. Oberthaler, R. Schmied, and P. Treutlein, *Rev. Mod. Phys.* **90**, 035005 (2018).
- [71] D. Petz and C. Ghinea, in *Quantum Probability and Related Topics* (World Scientific, Singapore, 2011).
- [72] L. Pezzè, M. Gabbriellini, L. Lepori, and A. Smerzi, *Phys. Rev. Lett.* **119**, 250401 (2017).
- [73] For instance,  $G(E_n) = 1$  for spin operators and eigenstates in the middle of the spectrum.
- [74] H. Araki, *Commun. Math. Phys.* **14**, 120 (1969).
- [75] J. R. Garrison and T. Grover, *Phys. Rev. X* **8**, 021026 (2018).
- [76] T. Kuwahara and K. Saito, *Phys. Rev. Lett.* **124**, 200604 (2020).
- [77] J. M. Deutsch, H. Li, and A. Sharma, *Phys. Rev. E* **87**, 042135 (2013).
- [78] L. Vidmar and M. Rigol, *Phys. Rev. Lett.* **119**, 220603 (2017).
- [79] C. Murthy and M. Srednicki, *Phys. Rev. E* **100**, 022131 (2019).

- [80] X.-L. Qi and D. Ranard, *Quantum* **3**, 159 (2019).
- [81] P. Zanardi, M. G. Paris, and L. C. Venuti, *Phys. Rev. A* **78**, 042105 (2008).
- [82] M. Gabbriellini, A. Smerzi, and L. Pezzè, *Sci. Rep.* **8**, 15663 (2018).
- [83] I. Frérot and T. Roscilde, *Phys. Rev. Lett.* **121**, 020402 (2018).
- [84] I. Frérot and T. Roscilde, *Nat. Commun.* **10**, 577 (2019).
- [85] C. N. Yang, *Rev. Mod. Phys.* **34**, 694 (1962).
- [86] P. Fendley, K. Sengupta, and S. Sachdev, *Phys. Rev. B* **69**, 075106 (2004).
- [87] I. Lesanovsky and H. Katsura, *Phys. Rev. A* **86**, 041601(R) (2012).
- [88] S. Choi, C. J. Turner, H. Pichler, W. W. Ho, A. A. Michailidis, Z. Papić, M. Serbyn, M. D. Lukin, and D. A. Abanin, *Phys. Rev. Lett.* **122**, 220603 (2019).
- [89] K. Bull, J.-Y. Desaulles, and Z. Papić, *Phys. Rev. B* **101**, 165139 (2020).